MULTI-TEMPORAL POLSAR BACKSCATTER DECOMPOSITION OVER GLACIER ICE, SNOW AND FIRN

Ian A. Brown [(1)]

[(1)] *Stockholm University, SE-106 91, Stockholm, Sweden, Email: Ian.Brown@natgeo.su.se*

ABSTRACT

A multi-temporal dataset of Radarsat-2 Quad-pol images from 2008-2011 was assembled over a Norwegian icecap, Blåmannsisen. Data were acquired in a range of imaging modes including FQ24 with a local incidence angle of 44° on the centre of the glacier and FQ3 with 21.5° at the same location. Scattering from the glacier facies was decomposed using Freeman-Durden and eigenvector-eigenvalue based approaches. Polarimetric discriminators were analysed to identify a temporal component to changes in backscatter and to identify the relative importance of incidence angle differences between acquisitions. It was found that any temporal signal was masked by strong differences associated with incidence angle effects. Polarimetric entropy and Freeman-Durden volume scattering were particularly strongly correlated with local incidence angle.

1. INTRODUCTION

Glacier monitoring is undertaken for climate change investigations or water resource management purposes. In Norway, glacier runoff is exploited for hydropower generation, supporting energy intensive industries and allowing the nation to export 14633 GWh of electricity to neighboring countries in 2009. Hydropower comprises 96% of the country‟s electricity generation in 2009 [1].

In situ and remote sensing approaches are used in glacier monitoring and may be considered complementary. Geophysical and proxy observations are common, particularly for mass balance estimation. Proxies for net surface balance may include observations of the end-of-summer snowline, other glacier surface facies and glacier surface changes [2], [3]. Synthetic aperture radar (SAR) observations of glacier surface facies are well described and the term radar facies may be used to describe the particular zonation observed in such data [4], [5]. SARs offer particular advantages over visible and infrared sensors, making high resolution observations independent of solar illumination or the presence of cloud. Furthermore, the penetration of GHz frequency SARs into dry snow means that such sensors can be used to obtain observations of sub-surface features such as the firn line during winter [4], [5]. The firn line is a proxy of time-integrated mass balance change, and may therefore indicate multi-annual trends in glacier mass balance [4].

Glacier surface facies describe the zonation of surface types such as the ablation facies, or dry snow facies, on a glacier or ice sheet [6]. The appearance of surface zones in SAR imagery has subsequently been termed the radar facies (or SAR facies) and is used to describe the variation in backscatter across homogenous or near homogenous regions [5]. Radar facies on a temperate glacier in the presence of liquid water near the surface, typically comprise of the wet snow facies and ablation facies. In the absence of liquid water the firn area is divided into the dry snow facies, where snow melt never occurs, whilst the percolation facies describes the zone in which snow melt occurs in summer and water percolates into the firn. Below this zone may be superimposed ice and the ablation or bare ice facies. The latter is the zone which experiences net ablation and lacks firn accumulation. Below the equilibrium line, in the ablation facies, surface scattering occurs at the air-snow interface and the snow-ice interface: volume scattering is assumed to be largely absent or low intensity, for example from layers and ice inclusions in the snowpack. Previous investigations have indicated that firn below the equilibrium line is indistinguishable from firn above the equilibrium line due to the similarity in backscatter mechanisms and the resultant backscatter intensity [3].

Scattering mechanisms on temperate glaciers, above the equilibrium line are normally assumed to comprise of surface scattering at the air-snow interface, and volume scattering from the snow and firn volume [7], particularly from ice inclusions [8]. In the case of a shallow snow-firn volume, surface scattering may also occur at the firn-ice interface at the base of the snow-firn volume. This scenario would require an abrupt transition from firn to ice resulting in a dielectric contrast to promote reflection [9]. In dry polar firn it has been hypothesized that scattering is dominated by surface scattering from layers in the firn [10] or from depth hoar [11]. This is a departure from models describing Rayleigh scattering from snow and firn grains, which are assumed to be spherical [9], [7].

These models were specifically developed to explain scattering from the Greenland ice sheet but should also be applicable to the other large ice sheets and icecaps a with dry snow zone. Uncertainties therefore remain

Proc. 'ESA Living Planet Symposium 2013', Edinburgh, UK
9–13 September 2013 (ESA SP-722, December 2013)

regarding scattering processes below the upper snow surface and the contribution of layers, inclusions and grains to backscatter amplitude. The depolarisation of waves in snow and firn is also poorly understood. Little has been published on the decomposition of backscatter from snow and firn. [12] investigated the co- and cross polarised backscatter responses from SIR-C and –X, and AIRSAR images over the Austrian Alps. They applied backscatter modelling to separate volume and surface scattering components but did not derive decompositions. In one of the few comprehensive analyses of PolSAR data over glaciers, [13] decomposed scattering in airborne SAR imagery into surface, volume and sastrugi components. They derived a specialised Freeman-Durden decomposition for glaciers. [14] derived Alpha, Entropy and Anisotropy decompositions from L- and P-band data over the Swiss Alps. They found strong relationships between polarimetric-interferometric (PolInSAR) measurements and firn temperature. No physical model was described to explain the scattering processes affected by firn temperature. That said, there are few analyses of scattering processes using polarimetric SAR data.

2. SITE DESCRIPTION

Blåmannsisen is an 87 km2 icecap in Fauske Kommune, northern Norway (Fig. 1). It is the fifth largest glacier in Norway. The icecap drains into Sweden on the eastern side and Norway on the western, northern and southern sides. All catchments are exploited for hydropower generation. Tunnels collect runoff from Blåmannsisen for the Siso power station north of the glacier. The drainage of lakes on the northeastern side have been affected by jökulhlaups caused by ice dam failures. One such jökulhlaup in 2001 drained 40 M m^3 of water in 35 hours into the reservoir below. No mass balance data from recent years exist for Blåmannsisen except one year of data from Rundvassbreen, the small northern outlet glacier

Blåmannsisen occupies a massif on the Vindfjell upland heath. The glacier has a southern dome which reaches approximately 1200 m.a.s.l and which is connected to a northern plateau by a broad saddle. The saddle and northern plateau include large regions with surface slopes below 5°. Much of the northern plateau is above 1300 m.a.s.l including a prominent peak, Blåmannen, which reaches over 1520 m.a.s.l.. On the eastern side of the saddle, Leirvatnbreen, is the largest and most gently sloping of the outlet glaciers. GPS measurements of surface elevation indicate the glacier is downwasting at a rate of approximately 1 m yr. The firn line in this region of the glacier is known to have retreated more than 1 km since the late 1990s [15]. The retreating EL has left a large region of exposed firn, interspersed with superimposed ice layers, below the current EL [15]. This region of the saddle and Leirvatnbreen are the focus of this investigation.

.

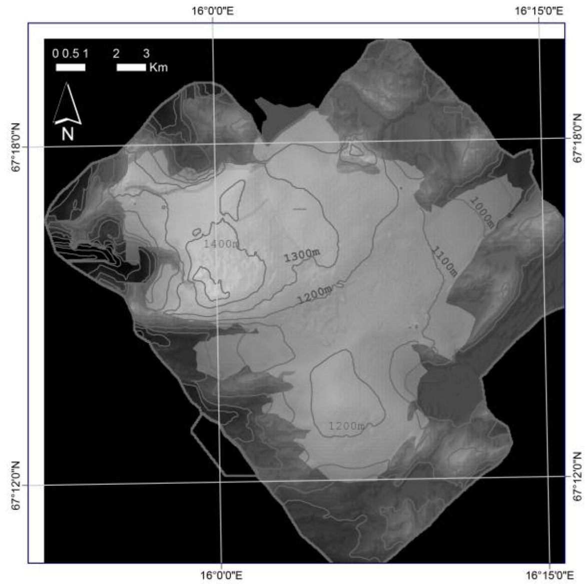

Figure 1. A Shaded relief map over the study site, Blåmannsisen. The approximate equilibrium line (EL) on Leirvatnbreen outlet glacier, to the east, is marked by the dashed line.

3. DATA AND METHODS

In total eight Radarsat-2 quad-pol image datasets were acquired during the dry snow season over the glacier (Tab. 1). Three images each from 2008 and 2011 and two from 2009. Ascending and descending passes were acquired; given the low surface slopes over much of the icecap these different pass orientations were not expected to affect backscatter in any meaningful way. Fine beam and standard beam modes were acquired from FQ3 to FQ24 and SQ5 to SQ11. Incidence angles over the equilibrium line (Fig. 1) ranged from 21-44°; all but one image were acquired with local incidence angles (LIAs) of 21-27°. The local surface slope at this location was 1°. All images were calibrated using an Ainsworth approach and were speckle filtered using a 7 x 7 modified Lee polarimetric speckle filter. Image products were geocoded with reference to a 15 m gridded digital elevation model (DEM) derived from a Tandem-X SAR image pair acquired in 2011.

In situ investigations at the site have been undertaken intermittently for 15 years. Ground penetrating radar profiles acquired at 800-2500 MHz in 2004 and 2007 indicate extensive layering in the firn near the EL. This layering occurs within a few metres of the previous summer surface. Cores taken using a PICO hand auger show layering in the firn, particularly at lower elevations. Below the EL a region of exposed firn was sampled. This region was characterised by interspersed layers of firn and superimposed ice of a total thickness of approximately 1 m above which dense, layered firn < 2 m thick was found. This firn, described as „old firn" is the remnant of the extensive firn line retreat that has occurred. This can be seen in optical imagery and is characterised by clear layering at the surface as successive summer surfaces are exposed.

Table 1. Parameters for the imagery used in this study

Date *yyyymmdd*	Mode	Ref. LIA[1] (Centre[2])	Pass
20080326	FQ3	21.5° (22)	Descending
20080402	FQ5	24.5° (24)	Descending
20080415	FQ3	22.6° (22)	Ascending
20090318	SQ10	29.0° (30)	Descending
20090320	SQ11	31.8° (31)	Ascending
20110318	SQ5	24.5° (24)	Descending
20110323	FQ24	43.6° (43)	Ascending
20110325	FQ8	27.4° (27)	Descending
Surface Slope	15 m DEM	1.2°	N/A

[1] *Reference point is 548310E 7460227N (1182 m.a.s.l.)*
[2] *Centre scene incidence angle in line of sight (LOS).*

4. RESULTS

A Freeman-Durden (FD) scatterer decomposition [16] was performed on the multi-temporal imagery using averages of 33 samples. The FD decomposition is a model based approach and has been shown to out-perform similar decompositions [17]. The FD decomposition estimates the contribution of double-bounce (DB), volume and rough surface scattering components of backscatter. Over firn regions below 1200 m the data from 2008 revealed a slight dominance of rough surface scattering (56-61%) with volume scattering of 37-41%. However, the imagery from 2009 and 2011 show an increase in volume scattering to 49-53% at shallower incidence angles rising to 67% in the FQ24 image from 2011. Surface scattering was 36-49% in the former datasets and 21% in the latter. Firn at higher altitudes exhibits higher surface scattering components and in the scenes from 2008 and one from 2009 surface scattering exceeds volume scattering. Over the older firn below the EL volume scattering dominated. In the 2011 imagery volume scattering accounted for 91-100% of total backscatter from this region. In the bare ice facies where firn is absent surface scattering was found to be dominant (57-70%) in all but two images. In two images from 2011 (FQ11 and FQ24) rough surface scattering accounted for 43 and 0% of backscatter, respectively.

In addition to the FD decomposition an eigenvector/eigenvalue based entropy-alpha-anisotropy decomposition was calculated for all datasets. Touzi discriminators derived from eigenvectors were also generated. Entropy can indicate whether the target is pure (a point target) or distributed. Low values indicate the former, values closer to 1 the latter [17]. Entropy increased between 2008 and 2011across the firn, „old firn" and bare ice facies. Anisotropy values between 0.4 and 0.65 were recorded over the „old firn" but were <0.26 over firn and bare ice. Both Entropy and alpha products exhibit an incidence angle dependency with higher values over larger local incidence angles. An additional measure, Touzi Psi [18], exhibits significantly higher values over „old firn" (35° to 40°) than firn (-20° to 3°) or bare ice (9 to 36°) for all descending pass images. Ascending images have a higher Touzi Psi response over ice than over other facies and do not seem to have a typical signature over „old firn" (though the sample size is only two).

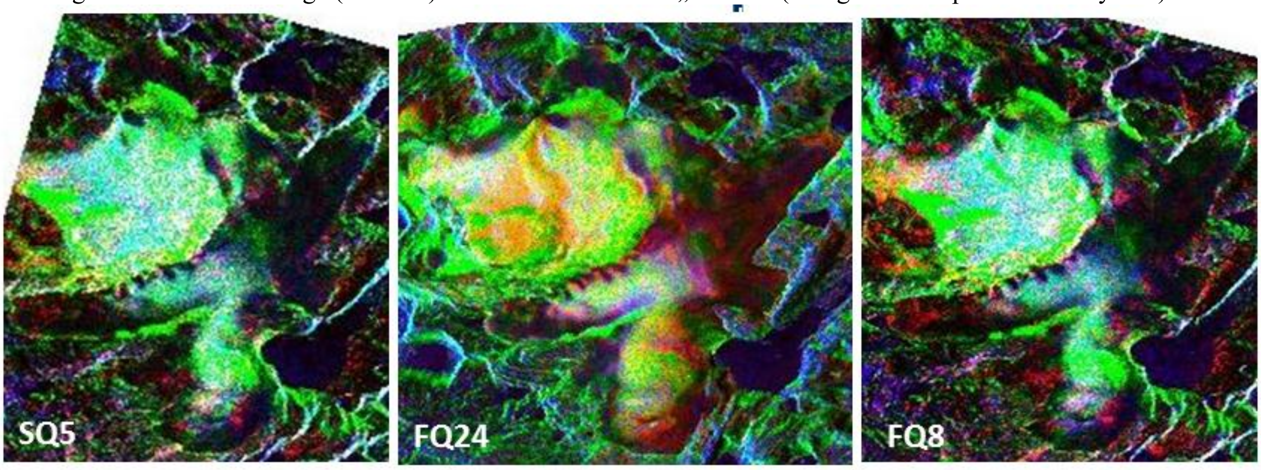

Figure 2. Freeman-Durden decompositions applied to three Radarsat-2 datasets from 2011 (18th March, 23rd March and 25th March, respectively).The image acquired in mode FQ24 displays a different pattern of scattering around the firn line. In the SQ5 and FQ8 images volume scattering dominates in the „old firn" region below the EL.

5. SUMMARY AND CONCLUSIONS

Entropy and volume scattering values over firn were found to be strongly correlated with the local incidence angle. Though the sample size was small (n=8) these results agree with scattering theory [9]. The relationship between these measures was strongest over the firn at lower elevations than that above 1300 m. However, the sampling site at higher elevations is more steeply angled to the east and hence LIA differences are likely to account for some of the differences between the two sampling sites and between ascending and descending pass images.

Entropy describes the randomness of the scattering problem with high values suggesting a scatterer ensamble and low values a point scatterer [17]. According to the H- $\bar{\alpha}$ plane the glacier facies are all moderately random scatterers. However, the $\bar{\alpha}$ component of the plane suggests zone 6 indicating random surface scattering. This contradicts the Freeman-Durden and Krogager (sphere-plane-dipole) decompositions. [17] note that there is a degree of arbitrariness in the zonation of the H- $\bar{\alpha}$ plane and it should be considered that in fact the firn and „old firn" are boundary cases that belong in zone 5:anisotropic particles. This would agree with the Rayleigh scattering model of volume scattering from ice particles in snow and firn and from ice inclusions. The presence of high anisotropy zones over „old firn" is likely to indicate the contribution of layering to backscatter.

No clear temporal pattern was found in the time series of imagery, despite the three year time span. It is possible that no significant changes have occurred within the individual facies: care was taken when sampling to ensure stable regions were used. The presence and absence of surface features such as sastrugi may complicate the temporal analysis of changes in scatterer composition. The range of acquisition modes used here also complicates image comparisons. Clearly for multi-temporal analyses data should be acquired using similar modes and the same pass direction. Nevertheless, the comparison between different modes has shown that higher incidence angles may improve our ability to define facies types and to monitor firn below the EL and thus the climate response of firn on temperate icecaps.

6. ACKNOWLEDGEMENTS

The author would like to thank MDA and the CSA for access to the Radarsat-2 imagery through the SOAR-EU program. Original images are copyright McDonald Detwiller Associates. The author would also like to acknowledge A. Reigber and M. Neumann and the Radar Tools development team whose software was used, and the Swedish National Space Board for financial support.

7. REFERENCES

[1] *Energi I Norge 2009*, The Norwegian Water Resources and Energy Directorate, Oslo, Norway, 2010.

[2] I.A. Brown, M.P. Kirkbride and R.A. Vaughan, "Find the firn Line! The suitability of ERS-1 and ERS-2 SAR data for the analysis of glacier facies on Icelandic icecaps". ***Int. J. Remote Sens.***vol. 20, no. 15-16, pp.3217-3230, 1999.

[3] D.K. Hall, R.S. Williams, J.S. Barton, O. Sigurdsson, L.C. Smith, and J.B. Garvin, "Evaluation of remote sensing techniques to measure decadal-scale changes of Hofsjökull ice cap, Iceland". ***J. Glaciol.***, vol. 46, no. 154, pp. 375-388, 2000.

[4] J.M. Ramage, B.L. Isaacs and M.M. Miller, "Radar glacier zones in southeast Alaska, USA: field and satellite observations", ***J. Glaciol.***, vol. 46, no. 153, pp. 287-296, 2000.

[5] R.V. Engeset, J. Kohler, K. Melvold, and B. Lundén, "Change detection and monitoring of glacier mass balance and facies using ERS SAR winter images over Svalbard". ***Int. J. Remote Sens.,*** vol. 23, no. 10, pp. 2023-2050, 2002.

[6] C.S. Benson, "Physical investigations on the snow and firn of Northwest Greenland 1952, 1953 and 1954" US Army Snow, Ice and Permafrost Research Establishment, Research Report 26, Sept. 1959. pp. 26.

[7] R.R. Forster, K.C. Jezek, J. Bolzan, F. Baumgartner and S.P. Gogineni, "Relationships between radar backscatter and accumulation on the Greenland ice sheet ", ***Int. J. Remote Sens.,*** vol. 20, no. 15-16, pp. 3131-3147, 1999.

[8] C. Mätzler, T. Strozzi, T. Weise, D. –M. Floricioiu and H. Rott, "Microwave snowpack studies made in the Austrian Alps during the SIR-C/X-SAR experiment", ***Int. J. Remote Sens.,*** vol. 18, no. 12, pp. 2505-2530, 1997.

[9] A.K. Fung, *Microwave scattering and emission models and their application.* Boston: Atrech House, 1994, ch. 9.

[10] E.W. Hoen and H.A. Zebker, "Penetration depths inferred from interferometric volume decorrelation observed over the Greenland ice sheet", *IEEE Trans. Geosci. Remote Sens.*, vol. 36, no. 6, pp. 2571-2583, Nov. 2000.

[11] S. Oveisgharan and H.A. Zebker, "Estimating snow accumulation from InSAR correlation observations", *IEEE Trans. Geosci. Remote Sens.,* vol. 45, no. 1, pp. 10-20, Jan 2007.

[12] D. Floriciou and H. Rott "Seasonal and short-term variability of multifrequency, polarimetric radar backscatter of alpine terrain from SIR-C/X-SAR and AIRSAR data", *IEEE Trans. Geosci. Remote Sens.*, vol. 39, no. 12, pp.2634 -2648 2001

[13] J. J. Sharma, I Hajnsek, K. P. Papathanassiou and A. Moriera. "Polarimetric decomposition over glacier ice using long-wavelength airborne PolSAR". *IEEE Trans. Geosci. Remote Sens.,* vol. 49, no.1, pp. 519-535.

[14] O. Stebler, A. Schwerzmann, M. Lüthi, E. Meier and D. Nüesch. "Pol-InSAR observations from an Alpine glacier in the cold infiltration zone at L- and P-band". *IEEE Geosci. Remote Sens. Lett.,* vol. 2, no. 3, 357-361. 2005.

[15] I.A.Brown, "Synthetic aperture radar measurements of a retreating firn line on a temperate icecap". *IEEE J. Selected Topics Earth Obs. Remote Sens.*, vol. 5, no. 1, pp. 153-160.2012.

[16] A. Freeman , and S.L. Durden "A three-component scattering model for polarimetric SAR data". *IEEE Trans. Geosci. Remote Sens*, vol. 63, no. 3. pp. 963-973. 1998.

[17] Lee, J.S., and Pottier, E. "Polarimetric Radar Imaging: From basics to applications", CRC Press, Rochester, New York., p. 397. 2009

[18] R. Touzi. " Target scattering decomposition in terms of roll-invariant target parameters". *IEEE Trans. Geosci. Remote Sens*, vol.45, no. 1. pp. 73-85. 2007.